Cellular and Molecular Life Sciences (2025) 82:7
https://doi.org/10.1007/s00018-024-05547-y

ORIGINAL ARTICLE

DNMT1 prolonged absence is a tunable cellular stress that triggers cell proliferation arrest to protect from major DNA methylation loss

Salvatore Martino[1] · Serena Gargano[1] · Pietro Salvatore Carollo[1] · Aldo Di Leonardo[1,2] · Viviana Barra[1]

Received: 23 July 2024 / Revised: 16 November 2024 / Accepted: 11 December 2024

Abstract

Methylation of cytosine in CpG dinucleotides is an epigenetic modification carried out by DNA-methyltransferases (DNMTs) that contributes to chromatin condensation and structure and, thus, to gene transcription regulation and chromosome stability. DNMT1 maintains the DNA methylation pattern of the genome at each cell cycle by copying it to the newly synthesized DNA strand during the S-phase. DNMT1 pharmacological inhibition as well as genetic knockout and knockdown, leads to passive DNA methylation loss. However, these strategies have been associated with different cell fates, even in the same cell background, suggesting that they can question the interpretation of the obtained results. Using a cell system in which endogenous DNMT1 is fused with an inducible degron and can be rapidly degraded, we found that in non-tumoral RPE-1 cells, DNMT1 loss progressively induced cell proliferation slowing-down and cell cycle arrest at the G1/S transition. The latter is due to p21 activation, which is partly mediated by p53 and leads to a global reduction in DNA methylation. DNMT1 restoration rescues cell proliferation, indicating that its deregulation is sensed as tunable cellular stress.

Keywords Epigenetics · Auxin-Inducible Degron · Genome stability · Cell cycle arrest · γH2AX

Abbreviations

DNMT1	DNA methyltransferase 1
DAC	2′-Deoxy-5-azacytidine
AZA	5-Azacytidine
AID	Auxin Inducible Degron
^{NA}DNMT1	mNeonGreen-AID-DNMT1
IAA	Indole Acetic Acid
EdU	5-Ethynyl-2′-deoxyuridine
5MeC	5-Methylcytosine
p21	p21waf1/cip1

Introduction

DNA methylation is an epigenetic mechanism that occurs mainly at CpG dinucleotides, which cells use to condense the chromatin. As such, it is involved in many cellular processes, including gene transcription regulation, embryonic development, X chromosome inactivation, gene imprinting, chromosome stability, and chromatin structure [1–8]. DNA methyltransferase 1 (DNMT1) is a DNA methyltransferase of maintenance since it preserves DNA methylation patterns by associating with replication foci and methylating hemimethylated DNA generated during each phase of DNA replication.

To investigate the critical role of DNMT1 further, various experimental approaches have been employed to impair its function, revealing its importance in genome stability. As observed by our laboratory and other groups, disabling DNMT1 function via treatments with 2'-deoxy-5-azacytidine (DAC) or 5-azacytidine (AZA), genetic knockout, or knockdown by RNA interference induces passive DNA demethylation after multiple cell cycles, DNA double-strand breaks, mitotic errors, and aneuploidy in both humans and mice [4, 9–13]. These results support the importance of DNMT1 in maintaining genome stability. Importantly, DNMT1 impairment usually leads to a reduction in cell proliferation, often culminating in cell cycle arrest and apoptosis, both in vivo and in vitro [10, 12, 14–16]. This is in agreement with DNMT1 being an essential gene [17–19]. However, cell behaviour and fate differ depending on the cell type and the strategy used to inhibit DNMT1. Clarifying the effects of

✉ Viviana Barra
viviana.barra@unipa.it

[1] Department of Biological, Chemical and Pharmaceutical Sciences and Technologies (STEBICEF), University of Palermo, 90128 Palermo, Italy

[2] Centro Di Oncobiologia Sperimentale (C.O.B.S.), Viale Delle Scienze, 90128 Palermo, Italy

Published online: 18 December 2024

DNMT1 depletion per se in normal human cells can provide important details on the functioning of DNMT1, elucidating whether and why DNMT1 is essential in differentiated cells. This could also have implications in cancer therapy, as DNMT1 inhibitors are used for the treatment of myelodysplastic syndrome (MDS) and hematological tumors, and the development of new ones is ongoing [20].

DAC and AZA have been widely used to inhibit DNMT1, as they are incorporated in the DNA to replace the cytosine and sequester DNMT1 by forming covalent bonds with it. Both drugs are able to induce DNA hypomethylation but they lead to different outcomes. Indeed, DAC induced G2-phase arrest in HeLa and HCT116 cell lines [21] while in A549 and T24 cells it led to G1-phase arrest and in KG1a cells to a subG1 arrest and an accumulation of cells in G2/M phase [11, 22, 23]. DAC was also able to induce G2-phase arrest with subsequent cell death and accumulation in the G2/M phase in MDS-L and MPM cell lines respectively [24, 25]. Surprisingly, AZA did not influence the cell cycle of the MDS-L cell line [25]: instead, it had an effect similar to that of DAC in KG1a cells causing accumulation of cells in the subG1-phase and apoptosis [11].

Chen et al. generated the DNMT1 conditional allele in HCT116 cells to evaluate the impact of DNMT1 inactivation. HCT116 cells, upon DNMT1 disruption, underwent G2-phase arrest that eventually resulted in a mitotic catastrophe [26], On the contrary, genetic knockout through homologous recombination in the same cell line did not affect cell growth as reported by Rhee and colleagues [27].

Similarly, exploring DNMT1's role in cell cycle progression through alternative methods, our laboratory observed by RNA interference that DNMT1 post-transcriptional silencing induced a G1-phase arrest in normal human fibroblasts IMR90 [12]. The silencing of DNMT1 in HCT116 cells, in contrast to the usage of DAC observed by Palii and colleagues, induced accumulation in the S-phase. DNMT1 silencing by a short hairpin in MPM cells only slightly increased the number of cells in the S-phase [24]. Finally, it was observed a proliferation arrest with increased cells in the S-phase in hepatocellular carcinoma upon DNMT1 post-transcriptional silencing [28]. Antisense oligonucleotides targeting DNMT1, instead, caused an intra-S-phase arrest in A549 cells [29], while they induced a severe reduction in the number of BrdU-positive cells in zebrafish posterior lateral line neuromasts [15].

Noncoding RNA can also directly regulate DNMT1 expression when overexpressed. DNMT1 targeting by mir342 has been demonstrated to induce a G1-phase arrest in SW480 cells [30].

The different effects observed upon DNMT1 impairment are probably the result of different genetic backgrounds (most of the cell lines used were tumoral) but also of the method used to disable DNMT1. Genetic disruption of DNMT1 might be too harsh, considering that DNMT1 is an essential gene, leaving the possibility for the cells to adapt depending on their genetic background. Post-transcriptional silencing on the other hand may be insufficient to efficiently deplete DNMT1 [12]. Also, the use of AZA or DAC, which are base analogs, is closely associated with side effects such as DNA damage [16, 31]. Thus, it is difficult to distinguish between the direct effect of the absence of DNMT1 protein/activity and secondary/side effects. To overcome this issue, we decided to use the non-tumoral cell line RPE-1 engineered to express the endogenous DNMT1 tagged with an Auxin-Inducible Degron (AID) [32]. The AID allows the rapid and complete degradation of DNMT1 (in approximately one hour) in the presence of auxin. Using this approach, we evaluated cell proliferation and activation of a cell cycle checkpoint. Altogether, our results demonstrate that DNMT1 is important for cell fitness, as its rapid degradation gradually leads to p53- and p21waf1/cip1-dependent cell cycle arrest at the G1/S transition in normal human cells. While the consequent passive DNA methylation loss has occurred, the restoration of DNMT1 can promote the reinitiation of cell proliferation.

Materials and methods

Cell culture

Retinal Pigment Epithelial cells (RPE-1), h-TERT immortalized, were previously engineered to express the F-box protein TIR1 and the endogenous DNMT1 tagged at N-terminus with AID (Auxin inducible degron) and mNeon Green (^{NA}DNMT1) [32]. Cells were cultured in Dulbecco's modified Eagle's medium (DMEM; Corning) supplemented with 10% bovine fetal serum and 1% L-Glutamine. Water soluble auxin indole-3-acetic acid sodium salt (IAA) (I5148; Sigma-Aldric) was used at 500 µM. This low concentration of IAA has been already documented not to affect RPE-1 cell growth [33, 34]. Cells were grown at 37 °C in a humidified atmosphere with 5% CO_2. For the IAA washout, RPE-1 ^{NA}DNMT1 cells were washed twice with 1X PBS and once with cell media.

Cell transfection

Cells were treated for 1 or 3 days with IAA to induce DNMT1 degradation and transfected as previously done [35]. The day before the transfection the cells were seeded in a 12-well plate. On the day of the transfection, specific siRNAs duplex (see the table below) were mixed with Lipofectamine 3000 Reagent (Invitrogen, Life Technologies) in Optimem media (Gibco), according to the manufacturer's recommendation, and added to the cells. At least after 5 h of incubation with

the siRNA mixture, the culture media was changed, and IAA was replaced every 2–3 days till day 4 or 6.

Target gene	siRNA sequence	References
p53	5′-GCA UGA ACC GGA GGC CCC AUtt-3′	[12]
Luc (control)	5′-CGTACGCGGAATACT TCGA-3′	[36]

Cell growth curves

Cells were seeded in 12 well plates and treated or not (control cells) with IAA for up to 7 days. At the indicated timepoints the cells were detached by trypsinization and counted with a Burker chamber. The experiment was performed in triplicate for each condition.

Immunoblot

Cells were collected by trypsinization, washed with PBS, and lysed in 1X Laemmli buffer (0.05 M Tris–HCl pH 6.8, 2% SDS, 10% glycerol, 0.01% bromophenol blue, 50 mM β-mercapto-ethanol) as previously performed [37]. The samples were loaded in a 10% polyacrylamide gel and blotted in a PVDF membrane. After 30 min of Blocking, the membranes were incubated with the following antibodies: DNMT1 (1:100, SantaCruz H-12: sc-271729), p21 (1:200; SantaCruz F-5: sc-6246), p53 (1:200; SantaCruz DO-1: sc-126) [38], phospho S15-p53 (1:1000; Abcam: ab1431), γH2Ax (1:500; Merck: 05-636), Vinculin (1:1000; Gene Tex: GTX109749-S), Actin (1:2000; Invitrogen: 5047778), GAPDH (1:5000; Proteintech: 80570-1-RR). The chemiluminescence signal was then visualized at the Bio-Rad ChemiDoc™ Imager and quantified with IMAGEJ. The experiment was performed in triplicate for each condition.

RTqPCR

RNA was extracted with TRIzol Reagent (Thermo Fisher Scientific) following the manufacturer's instructions.

Purified RNA was then quantified using Nanodrop™ and loaded on 1% agarose gel to verify its integrity. For each sample, 1 µg of RNA was reverse-transcribed using the High-Capacity cDNA Reverse Transcription Kit (Thermo Fisher Scientific, Milan, Italy) with the following conditions, according to the manufacturer's instructions:

	Step 1	Step 2	Step 3	Step 4
Temperature (°C)	25	37	85	4
Time	10 min	120 min	5 min	∞

RT-qPCR was performed using Applied Biosystems 7300 Real-Time PCR System as previously described [39]. Briefly, each sample was amplified in triplicate (50 ng of cDNA/sample) in a final volume of 15 µL 1X Master Mix SyBR Green (Thermo Fisher Scientific, Milan, Italy) supplemented with 150 nM primer mix and with the following thermal cycle: 95 °C for 15 s, 60 °C for 60 s repeated for 40 cycles. Relative gene expression was quantified by comparing the $2^{-\Delta\Delta Ct}$ of each analyzed gene to that of the *GAPDH* gene used as the internal control. The experiment was performed in triplicate for each condition. The used primers are indicated in the following table:

$p21^{waf1/cip1}$ Forward primer	5′-CTGGAGACTCTCAGGGTC GA-3′
$p21^{waf1/cip1}$ Reverse primer	5′-CGGATTAGGGCTTCCTCT TG-3′
GAPDH Forward primer	5′-CTCATGACCACAGTCCAT GCC-3′
GAPDH Reverse primer	5′-CAATCCACAGTCTTCTGG GT-3′
p14ARF Forward primer	5′-TGATGCTACTGAGGAGCC AGC-3′
p14ARF Reverse primer	5′-AGGGCCTTTCCTACCTGG CTC-3′

Cell cycle analysis by flow cytometry

Cell cycle analysis was conducted as previously done [40]. Briefly, after the indicated treatment asynchronously growing cells were collected in PBS, then fixed in 70% ice-cold ethanol and incubated at 4 °C at least overnight. On the day of the analysis, cell pellet was resuspended in Propidium Iodide/RNase staining buffer in the dark (20 µg/mL PI and 40 µg/mL RNase) and incubated for at least 30 min. The samples were acquired on FACSAriaIII by AteN Center, University of Palermo. Experiments were repeated twice and at least 10,000 events were analysed for each sample. Flow cytometry data were then analyzed with FCS Express 7 (De Novo Software).

Click-iT EdU imaging

S phase evaluation was performed using the Click-iT Plus EdU Alexa Fluor 555 Imaging Kit (Invitrogen, C10638) following the manufacturer's instructions. Cells were seeded on round glass coverslips in a 12-well plate and treated (or not) with the hormone IAA. On the day of the analysis, cells were incubated with EdU (10 µM). After 2 h of incubation, cells were fixed with 3.7% formaldehyde in 1X PBS for 15 min at room temperature and permeabilized with 0.5% Triton X-100 in 1X PBS for 20 min at room temperature. All the washing steps were performed with 3% BSA in 1X PBS. A

click reaction was catalyzed to label and detect the EdU: cells were incubated with the Click-iT Plus reaction cocktail for 30 min at room temperature, protected from light. Nuclei were counterstained with Hoechst 33342 (5 µg/mL). The slides were mounted with ProLong™ Gold Antifade Mountant (Thermo Fisher Scientific) and cells were imaged using a 10× and a 63× objectives in a Zeiss Axioskop microscope.

Mitotic index evaluation

Cells were harvested and collected with PBS. Cell pellets were then resuspended drop by drop at vortex with pre-warmed 75 mM KCl hypotonic solution and incubated at 37 °C for up to 20 min. After the incubation, cell pellets were fixed at least 3 times with cold Carnoy fixative (3:1, Methanol: Glacial Acid Acetic). The samples were dropped onto cold glass slides and left to air dry overnight. Once dried, the slides were stained with 3% Giemsa Gurr staining solution and then observed at an up-right microscope with transmitted light with 20× magnification. At least 10 images were taken for each condition to evaluate the mitotic index (number of mitoses/total number of cells). The experiment was performed as three independent replicates.

Immunofluorescence assays

MPM2

MPM2 staining was performed as previously [41]. Cells were seeded onto glass slides. On the day of the analysis, the cells were washed with 1X PBS and fixed on ice with cold methanol for 5 min. The methanol was then discarded, and the cells were washed 3 times with 1X PBS. The cells were then blocked for 1 h with 1% BSA diluted in PBS and then incubated overnight at 4 °C with antibodies anti-MPM2. (1:100; Merck, Milan, Italy, 05-368). The next day, the cells were washed with PBS, and then incubated for 1.5 h at 37 °C with the secondary antibody 1:1000 anti-mouse Cy3-conjugated (Jackson ImmunoResearch; 715-225-150) in 1X PBS. Nuclei were then counterstained with DAPI for 3 min, the slides were mounted with ProLong™ Gold Antifade Mountant, and cells were imaged with a Zeiss Axioskop microscope.

5-Methylcytosine

Cells were grown onto coverslips, then washed with 0.1% Tween-20 in PBS and fixed with 4% formaldehyde in PBS for 10 min in the dark. Upon fixation, the cells were permeabilized with 0.5% Triton x-100 diluted in PBS for 30 min and then, treated with 2 M HCL for 30 min at room temperature. After washing with 0.1% Tween-20 in PBS and blocking for 1 h with 2% BSA in 1% Tween-20 in PBS, cells were incubated with the primary antibody anti-5-Methylcytosine (5MeC) (1:500; Epigentek, Farmingdale, NY, USA, clone 33D3; A-1014) overnight at 4 °C. The cells were then washed and incubated with 1:500 anti-mouse Cy3-conjugated in 0.1% Tween-20 in PBS for 1 h at 37 °C. After washing 3 and counterstaining with DAPI for 3 min, the slides were mounted with ProLong™ Gold Antifade Mountant and observed with Zeiss Axioskop microscope.

Statistical analysis

For all the performed sets of experiments, we applied statistical analysis by using Prism software (GraphPad). As indicated in the Figure legends, the statistical significance of comparisons between two samples or experimental conditions was assessed by the two-tailed unpaired Student's t-test. For the proliferation curve in Fig. 1B, instead, we used a 2way ANOVA test. We generally assumed a standard normal distribution, but this was not formally tested. We considered it significant if the calculated P value was < 0.05. P values were indicated as follows: *$P < 0.05$; **$P < 0.01$; ***$P < 0.001$; ****$P < 0.0001$; ns = not significant.

Results

Prolonged DNMT1 absence induced proliferation defects and cell cycle arrest in the G1-S phase of the cell cycle in normal human cells

To study DNA hypomethylation effects on normal cells, we took advantage of the RPE-1 cell line (Retinal Pigment Epithelial cells) engineered to express endogenous DNMT1 tagged with both mNeonGreen and auxin-inducible degron AID (RPE-1 ^{NA}DNMT1) [32]. Upon the addition of auxin indole Acetic Acid (IAA), the system allowed DNMT1 degradation (Fig. 1A, Suppl. Fig. 1A, B). Nevertheless, by live microscopy observation, we found that approximately 0.8% of the cells did not respond to IAA (escapers) (data not shown), which could be responsible for the low residual level of DNMT1 in the immunoblot (Suppl. Fig. 1B).

We first assessed DNMT1's importance in cell proliferation and cell cycle over a timeframe of 7 days upon IAA treatment. RPE-1 ^{NA}DNMT1 cells underwent a progressive slowing-down in cell proliferation, which became significant over time (Fig. 1B). To ensure that the presence of escapers in the cell population did not alter our results, we analyzed the growth of one clone obtained from a single cell of the population (clone5). The clone5 treated with IAA showed a slowing down of cell proliferation as well as the entire population (Supp. Fig. 1C).

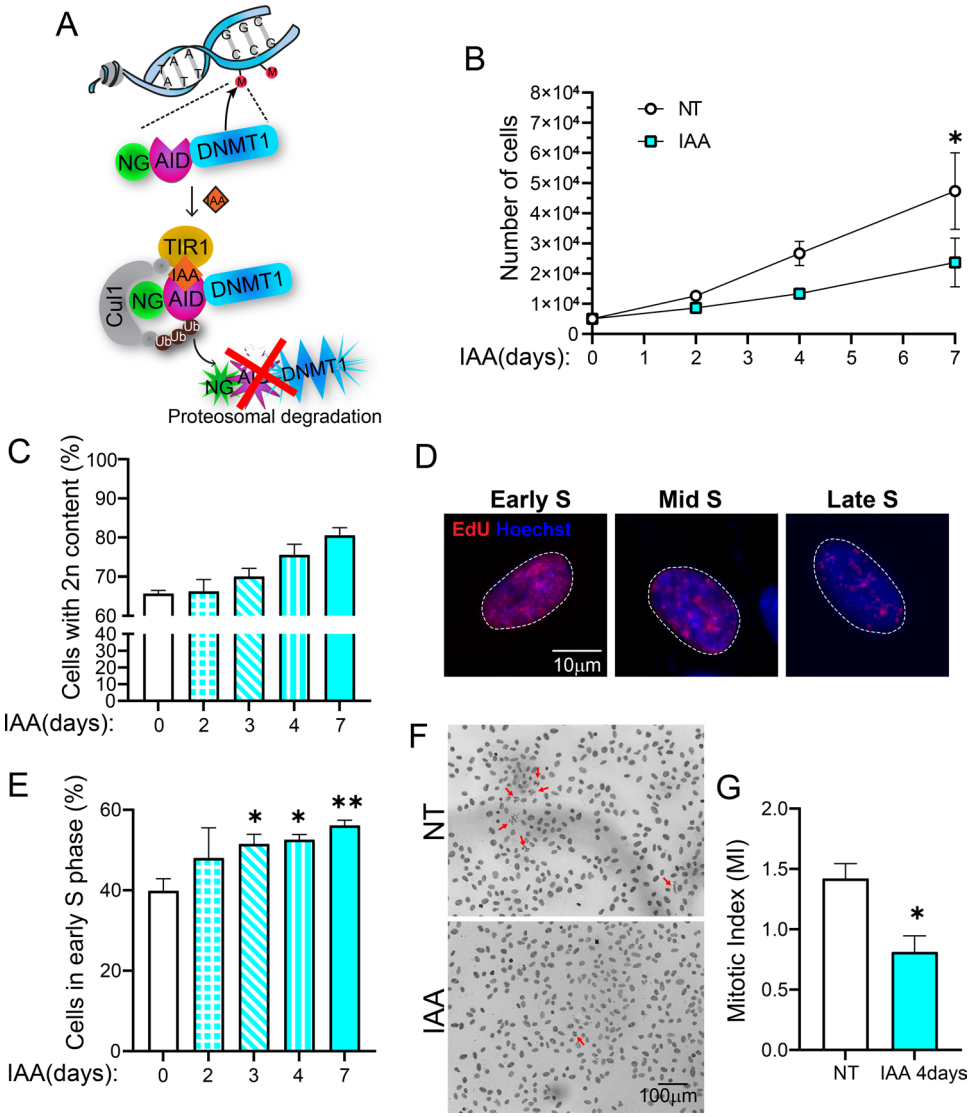

Fig. 1 Antiproliferative effect of DNMT1 degradation. **A** Schematics of ^{NA}DNMT1 degradation due to AID system, in the presence of IAA. **B** Cell growth curves showing the proliferation defects of IAA-treated RPE-1 ^{NA}DNMT1 cells in respect to the untreated ones. The graph shows the mean of 3 independent experiments. The error bars represent the standard error of the mean, SEM. 2way ANOVA between the samples: $*\leq 0.05$; ns > 0.05. **C** Histogram summarising flow cytometry analysis of Propidium Iodide-stained cells showing the increased percentage of IAA-treated RPE-1 ^{NA}DNMT1 cells with 2n DNA content. The graph shows the mean of 2 independent experiments. **D** Representative images of immunostaining for EdU (red) showing the differences between the S phase stages (early S, mid-S, late S). Nuclei were counterstained with Hoechst. **E** Quantification of RPE-1 ^{NA}DNMT1 cells (treated or not with IAA) positive for EdU showing the accumulation of cells in the early S phase starting from 3 days of treatment. The graph shows the mean of 3 independent experiments. At least 150 nuclei for each condition were evaluated. The error bars represent the standard error of the mean, SEM. Unpaired t-test between the samples: $**<0.01$; $*\leq 0.05$; ns > 0.05. **F** Representative images of mitotic spreads of untreated and IAA-treated RPE-1 ^{NA}DNMT1 cells. The nuclei and chromosomes were stained with Giemsa. Red arrows point to cells in mitosis. **G** Mitotic index quantification of untreated and 4-day IAA-treated RPE-1 ^{NA}DNMT1 cells. The graph shows the mean of 3 independent experiments; at least 150 nuclei were analyzed for each sample. The error bars represent the standard error of the mean, SEM. Unpaired t-test between the samples: $*\leq 0.05$; ns > 0.05

To assess whether the observed slow cell proliferation was due to cell cycle arrest, flow cytometry analysis with Propidium Iodide staining was performed. The histogram in Fig. 1C shows the progressive accumulation of cells with 2n DNA content starting from the third day of treatment. This result suggests possible cell cycle arrest in the G1 phase or at the G1/S transition. To quantify cells actively replicating DNA (S phase) EdU assay was performed on RPE-1 ^{NA}DNMT1 cells upon IAA treatment. As shown in Supp. Fig. 1D, the percentage of cells in the S phase did

not change in IAA-treated cells compared with that in the untreated control. However, we took advantage of the pattern of the incorporated EdU to identify cells in different stages of the S phase [42] (Fig. 1D). The graph in Fig. 1E reveals a significant increase in the percentage of cells in the early S phase, starting from the third day of treatment (Fig. 1E, Supp. Fig. 1E), which is consistent with the accumulation of cells with a 2n DNA content (Fig. 1C). To further confirm this, we synchronized the cells in the G1 phase (2n DNA content) by serum starvation for 48 h, and then released the cells in the presence or absence of IAA for an additional 4 and 6 days (Supp. Fig. 2A), and evaluated the cell cycle progression with flow cytometry (Supp. Fig. 2B). These results showed that once synchronized, RPE-1 ^{NA}DNMT1 cells had mainly a 2n DNA content (~ 80%) after release in IAA for 4 and 6 days (Release IAA 4d and 6d). In contrast, the cells released for 4 days in normal media (Release NT) re-entered the cell cycle with a profile similar to that of asynchronous cells (NT async).

Taken together, these results strongly suggest that RPE-1 ^{NA}DNMT1 cells arrest their proliferation at the G1/S transition when DNMT1 absence is prolonged.

To confirm the cell cycle arrest of RPE-1 ^{NA}DNMT1 cells, the mitotic index was also evaluated (Fig. 1F) which showed a significant reduction in the RPE-1 ^{NA}DNMT1 cell population in mitosis after 4 days of IAA treatment (Fig. 1G).

Cell cycle arrest induced by DNMT1 prolonged absence is due to p21 p53-dependent activation

It was previously observed that DNMT1 acute depletion induces activation of the p53-p21(waf1/cip1) pathway via p14ARF upregulation [12]. Similarly, we observed an increase in p21, both at the transcriptional and protein levels, in RPE-1 ^{NA}DNMT1 cells from the third day of treatment (Fig. 2A, B, D). Instead, while the total fraction of p53 protein did not change upon the treatment (Suppl. Fig. 1F), the fraction of activated p53 phosphorylated at S15 increased from the fourth day of IAA treatment (Fig. 2A and C). However, the p14ARF transcript level increased only on the 7th day of treatment (Suppl. Fig. 1G), suggesting that its activation and involvement in p53 and p21 triggering is not an early event following DNMT1 protein degradation.

To test the involvement of p53 in p21 upregulation, we knocked down p53 by RNA interference during IAA treatment (Fig. 2E). Following p53 reduction, the p21 protein increase in IAA-treated cells was reduced (from 2.2 of IAA siLuc to 1.5 of IAA sip53) (Fig. 2F–G and Suppl. Fig. 1H). However, the p21 protein level was not lowered down to that of the untreated condition, suggesting that either the residual p53 (Fig. 2F) keeps activating p21, or p53 could not be the only regulator of p21 activation in a DNMT1-depleted context. Nevertheless, MPM2 staining revealed that, while only 1.7% of RPE-1 ^{NA}DNMT1 control cells treated with IAA were in G2 phase/mitosis (G2/M) (in accordance with the mitotic index shown in Fig. 1G), 8.7% of the p53-depleted cells (sip53) were in G2/M when treated with IAA (Fig. 2H, I). Importantly, the percentage of IAA-treated RPE-1 ^{NA}DNMT1 sip53 cells in the G2/M was similar to that of the untreated control cells (Fig. 2I). These data indicated that p53 reduction was sufficient to rescue the proliferation arrest observed following DNMT1 prolonged degradation.

DNMT1 rescue restores normal levels of p21 and cell proliferation arrest

We then sought to evaluate whether or not cell proliferation defects were reversible. We, thus, washed out IAA and checked the effect of ^{NA}DNMT1 rescue after 24 h (Fig. 3A, B and Supp. Fig. 2C). We observed the reduction of p21 protein in the washout (WO) condition with respect to both IAA- and untreated samples suggesting that DNMT1 recovery even for only 24 h is sufficient to shut down p21 activation (Fig. 3C, D).

We, then, analyzed EdU staining and observed no significant difference in the percentage of cells in the S phase or early S after IAA washout with respect to the untreated cells, suggestive of no changes in the cell cycle progression (Fig. 3E and Supp. Fig. 2D). However, the reduction of the percentage of washed-out cells in the early S phase was not statistically different from the one of IAA treatment, probably suggesting that 1 day of DNMT1 rescue might be not enough to completely recover the G1/S arrest.

To have a better understanding of the progression of the cell cycle after IAA washout, we evaluated G2 and mitosis. MPM2 staining showed no significant difference in the percentage of cells in G2/M between the washout and the untreated samples, suggesting a recovery of cell proliferation when DNMT1 is restored (Fig. 3F). However, there was no significant increase in the percentage of cells in G2/M between the washout and the IAA-treated conditions (Fig. 3F). On the other hand, by analyzing the mitotic index, we observed a full recovery of the cells in mitosis after IAA washout with respect to the IAA treatment (Fig. 3G, H). Also, the mitotic index was comparable to the one of untreated RPE-1 ^{NA}DNMT1 cells. To evaluate the possibility that 1 day of release from IAA might be not enough to fully restore the cell cycle, we repeated the experiments on the RPE-1 ^{NA}DNMT1 cells clone5 extending the wash out to 2 days and we named this condition WO2d (Supp. Fig. 2E). Immunoblotting confirmed the complete rescue of DNMT1 (Supp. Fig. 2F) and MPM2 staining also revealed a significant increase in the percentage of cells in G2/M upon two days of release from IAA (WO2d) with respect

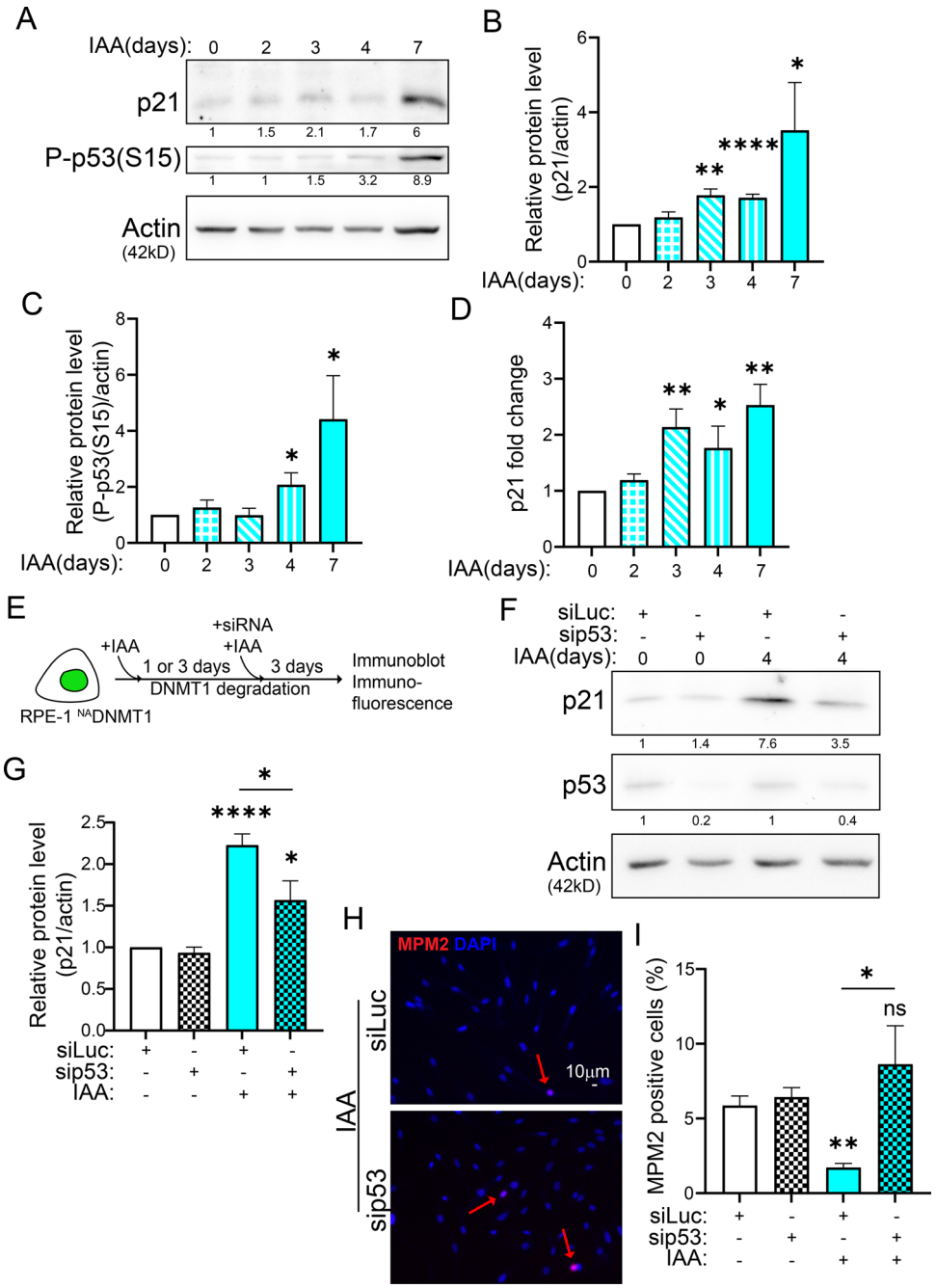

Fig. 2 DNMT1 degradation induces cell proliferation arrest that is dependent on p53 and p21. **A** Immunoblot showing the level of p21 protein and phosphorylated p53 on serine 15 (P-p53(S15)) at the indicated time points during IAA treatment. **B** Quantification of **A** showing p21 increase during IAA treatment. The graph shows the mean of at least 3 independent experiments. The error bars represent the standard error of the mean, SEM. Unpaired t-test between the samples: **** < 0.0001; ** < 0.01; * ≤ 0.05. **C** Quantification of **A** showing P-p53(S15) increase upon IAA treatment. The graph shows the mean of at least 3 independent experiments. The error bars represent the standard error of the mean, SEM. Unpaired t-test between the samples: * ≤ 0.05. **D** Histogram summarising RT-qPCR results of p21 transcript levels in RPE-1 ^{NA}DNMT1 cells during IAA treatment. The graph shows the mean of at least 3 independent experiments. The error bars represent the standard error of the mean, SEM. Unpaired t-test between the samples: ** < 0.01; * ≤ 0.05. **E** Schematics showing how sip53 experiments were performed. **F** Representative immunoblot of p21 and p53 in the indicated samples. **G** Graph summarising the results of **F** shows that sip53 transfection reduces p21 protein level in RPE-1 ^{NA}DNMT1 cells upon IAA treatment. The graph shows the mean of at least 3 independent experiments. The error bars represent the standard error of the mean, SEM. Unpaired t-test between the samples: **** < 0.0001; * ≤ 0.05. **H** Representative images of immunofluorescence assay targeting MPM2 in IAA-treated RPE-1 ^{NA}DNMT1 cells transfected with siLuc (control) or with sip53. Nuclei were counterstained with DAPI. **I** The graph is the quantification of **H**. The graph shows the mean of 3 independent experiments. At least 100 nuclei for each sample were evaluated. The error bars represent the standard error of the mean, SEM. Unpaired t-test between the samples: ** < 0.01; * ≤ 0.05; ns > 0.05

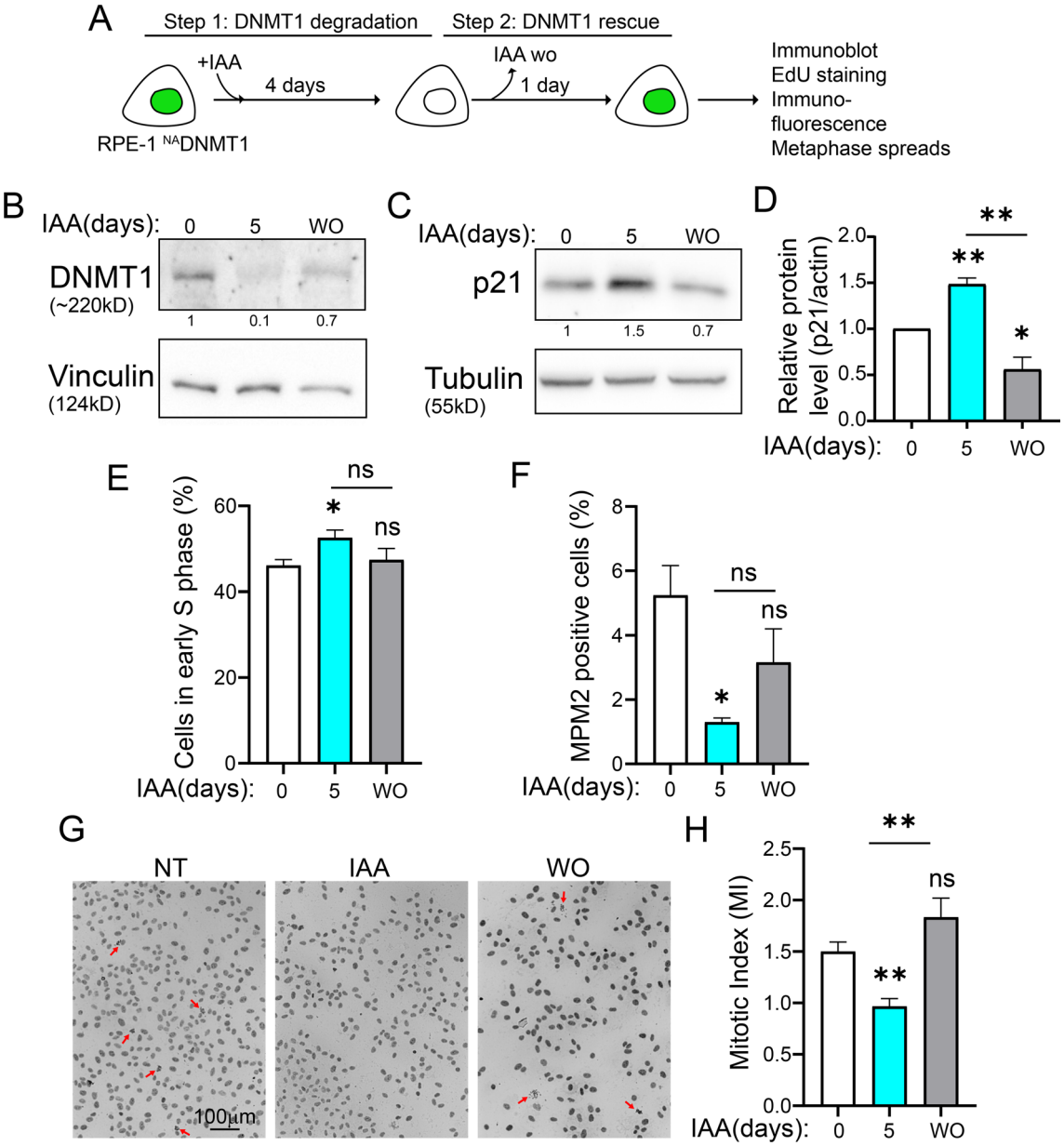

Fig. 3 DNMT1 restoration rescues cell proliferation. **A** Schematics showing how washout experiments were performed. **B** Immunoblot shows ^{NA}DNMT1 successfully recovered upon 1 day of IAA washout. **C** Immunoblot of p21 level in the untreated, IAA-treated, and washed-out RPE-1 ^{NA}DNMT1 cells. **D** Graph summarising the results in **C** highlights that ^{NA}DNMT1 rescue reduces p21 level in RPE-1 ^{NA}DNMT1 cells. The graph shows the mean of 3 independent experiments. The error bars represent the standard error of the mean, SEM. Un-paired t-test between samples ** < 0.01; * ≤ 0.05; ns > 0.05. **E** Graph summarising EdU staining data in the washout experiments. The graph shows the mean of 3 independent experiments. The error bars represent the standard error of the mean, SEM. At least 200 nuclei for each condition were evaluated. Unpaired t-test between samples: * ≤ 0.05; ns > 0.05. **F** Graph summarising data of MPM2 staining in the untreated, IAA-treated, and washed-out conditions. MPM2-positive cells increase after ^{NA}DNMT1 rescue. The graph shows the mean of 3 independent experiments. At least 150 cells were analyzed for each sample. The error bars represent the standard error of the mean, SEM. Unpaired t-test between the samples: * ≤ 0.05; ns > 0.05. **G** Representative images of mitotic spreads of untreated, IAA-treated, and washed-out RPE-1 ^{NA}DNMT1 cells. The nuclei and chromosomes were stained with Giemsa. Red arrows indicate cells in mitosis. **H** Graph summarising the data in **G**. Increased mitoses are observed in the IAA-washout condition. The graph shows the mean of 3 independent experiments. The error bars represent the standard error of the mean, SEM. At least 450 cells were evaluated. Unpaired t-test between the samples: ** < 0.01; ns > 0.05

to the IAA-treated condition (Supp. Fig. 2G). These results suggest that the proliferation arrest induced by prolonged DNMT1 absence can be progressively rescued by DNMT1 restoration.

DNMT1 inducible degradation causes global DNA demethylation

To evaluate whether DNMT1 inducible degradation affects global DNA methylation levels, a 7-day time-course analysis was carried out on RPE-1 ^{NA}DNMT1 cells (Fig. 4A, B). Similar to previous observations in DLD-1 ^{NA}DNMT1 cells [32], 5-methylcytosine (5MeC) immunostaining showed a progressive reduction in global DNA methylation starting from 2 days after IAA addition. The maximum degree of methylation loss is reached after 4 days of treatment, remaining unchanged up to 7 days of treatment. This finding is in accordance with the G1/S cell cycle arrest at both 4 and 7 days after IAA addition (Fig. 1C, E).

Given the association between global DNA demethylation and DNA damage signaling [11, 16, 43], we also wanted to address whether decreased levels of 5MeC could possibly trigger phosphorylation of histone H2AX on serine 139 (γH2AX), one of the earliest markers of the DNA damage response. However, we did not find any increase of γH2AX by immunoblotting (Supp. Fig. 2H), as we previously reported [12], suggesting no occurrence of DNA damage.

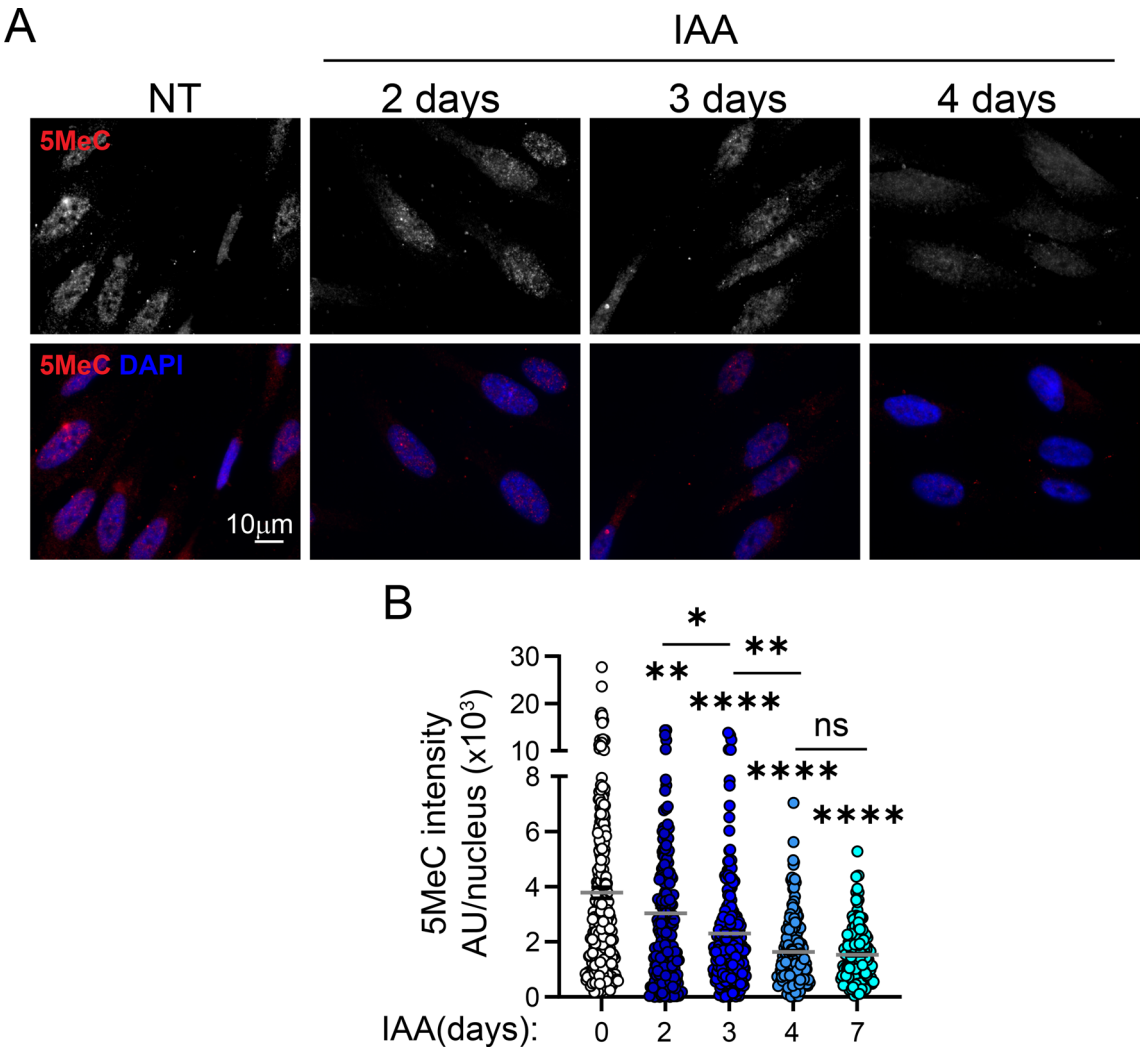

Fig. 4 DNMT1 inducible degradation causes global DNA demethylation. **A** Representative images of immunostaining for 5-Methyl-Cytosine (5MeC) displaying global DNA methylation reduction from 2 days up to 4 days of IAA treatment. Nuclei were counterstained with DAPI. **B** Single-cell nucleus quantification of 5MeC signal (AU: arbitrary unit) without (0 days) or with IAA (2, 3, 4 and 7 days) treatment. The scatter plot is cumulative of 6 independent experiments with at least 150 cells counted for each condition. Error bars represent the standard error of the mean SEM. Un-paired t-test between the samples: **** < 0.0001; ** < 0.01; * ≤ 0.05; ns > 0.05

Discussion

Studies on the role of DNMT1 in cell fitness, defined as the cells' ability to thrive in a specific environment, have shown varying results even within the same genetic background, making it challenging to determine its true importance in normal cells. These results might be due to the systems used to disable DNMT1. Here, we employed a cell model that we have recently published where DNMT1 endogenous protein can be rapidly and completely degraded using an inducible degron [32] in the non-tumoral RPE-1 cell line. This approach allows us to observe the direct and immediate effects of the protein absence in normal cells without potential biases from cytotoxicity caused by DNMT1-inhibiting drugs or siRNA transfection, or from cell adaptation to the gene knockout. We observed a gradual decrease in cell proliferation, culminating in a block occurring at the G1/S transition between days 4 and 7 in the absence of DNMT1. This suggests that DNMT1 protein is dispensable for cell proliferation for a few cell cycles (approximately 3–4 cell cycles), but its prolonged absence triggers a cell cycle arrest at the G1/S transition, inhibiting cells from replicating their DNA. In parallel, as the cells proliferate in the absence of DNMT1, passive DNA demethylation occurs and reaches its peak by day 4. This suggests that this methylation level may represent the maximum tolerance for maintaining the normal progression of the cell cycle. Indeed, major changes in both cell proliferation and cell cycle occur starting from day 4. However, upon restoring DNMT1 protein through IAA washout, cells exit the proliferation arrest and begin re-entering mitosis within 24 h, indicating that DNMT1 presence is perceived as a solution to restore cell proliferation. This observation could also imply that ensuring the maintenance of the minimal tolerable level of DNA methylation through rescued DNMT1 activity is sufficient to allow cell cycle progression. The minimal tolerable level of DNA methylation might constitute the threshold to avoid unrecoverable and dangerous genetic instability [6].

We also investigated the checkpoint triggered by DNMT1 prolonged absence and DNA methylation loss. Interestingly, despite the different types of arrest in the cell cycle observed so far in the previous literature, DNMT1 impairment often triggers the activation of cyclin-dependent kinase inhibitors, mainly p21 [12, 21, 24, 30, 44, 45]. We previously demonstrated that p21 activation and consequent cell cycle arrest is an immediate event in response to DNMT1 acute depletion in normal primary fibroblasts [12]. With the inducible degradation of DNMT1, we confirmed p21 activation even though it is not an immediate response but rather a delayed response to DNMT1's prolonged absence and DNA methylation loss. We also demonstrated that p21 activation is mostly triggered by p53 which is predominantly phosphorylated on serine 15, a marker of a stabilized and active p53 that cannot be inhibited by MDM2 [46]. Knocking-down of p53, as a consequence, releases cell proliferation arrest. Interestingly, p14ARF, which we previously showed to be responsible for the cell cycle arrest in the case of acute DNMT1 depletion by RNA interference, is activated only at day 7 in the absence of DNMT1. This activation likely occurs when DNA methylation conditions become critically compromised, necessitating stricter regulation of the cell cycle. Also, we did not observe an increase of γH2AX suggesting the occurrence of DNA damage that could have triggered p53 phosphorylation and activation, as previously reported [12].

Altogether, our results demonstrate that the prolonged absence of DNMT1 and consequent DNA methylation loss act as cellular stress signals that can endanger genome stability. This triggers p53-dependent p21 activation to halt cell proliferation before methylation reaches critical low levels. Notably, this proliferation arrest can be reversed when the stress source—such as DNMT1 loss—is resolved by restoring DNMT1 protein levels. Future research is needed to identify the specific cellular sensor responsible for detecting this stress and to explore whether this sensor can be modulated. This line of investigation could be particularly significant given that DNA methylation loss is a hallmark of numerous human diseases, including cancer. Understanding this stress-response pathway, and how it intersects with the fundamental processes of cell cycle control and genomic stability, could ultimately open new therapeutic avenues to target abnormal cell proliferation, offering hope for more effective treatments against diseases associated with DNA methylation loss.

Supplementary Information The online version contains supplementary material available at https://doi.org/10.1007/s00018-024-05547-y.

Acknowledgements We wish to thank Daniele Fachinetti, Institut Curie (Paris, France) for sharing and agreeing to the use of the engineered cells and for his helpful comments, and ATeN Center, University of Palermo (Italy), for acquiring flow cytometry data.

Author contributions Conceptualization: V.B.; Methodology: V.B. and A.D.L.; Formal analysis and investigation: S.M., S.G., P.S.C.; Writing—original draft preparation: V.B. and S.M.; Writing and editing: V.B., S.M., S.G., P.S.C.; Commenting draft: V.B. and A.D.L.; Supervision: V.B..

Funding This work was supported by FFR2023 and FFR2024 to VB.

Data availability The data that support the findings of this study are available within the article and its supplementary materials. Additional details are available from the corresponding author on request.

Declarations

Conflict of interests The authors have no relevant financial or non-financial interests to disclose.

Consent for publication All authors reviewed the results and contributed to the final manuscript. All authors approved this manuscript for publication.

References

1. Illingworth RS, Bird AP (2009) CpG islands—'A rough guide.' FEBS Lett 583:1713–1720. https://doi.org/10.1016/j.febslet.2009.04.012
2. Choy JS, Wei S, Lee JY et al (2010) DNA methylation increases nucleosome compaction and rigidity. J Am Chem Soc 132:1782–1783. https://doi.org/10.1021/ja910264z
3. Sharp AJ, Stathaki E, Migliavacca E et al (2011) DNA methylation profiles of human active and inactive X chromosomes. Genome Res 21:1592–1600. https://doi.org/10.1101/gr.112680.110
4. Sheaffer KL, Elliott EN, Kaestner KH (2016) DNA hypomethylation contributes to genomic instability and intestinal cancer initiation. Cancer Prev Res (Phila) 9:534–546. https://doi.org/10.1158/1940-6207.CAPR-15-0349
5. Tucci V, Isles AR, Kelsey G et al (2019) Genomic imprinting and physiological processes in mammals. Cell 176:952–965. https://doi.org/10.1016/j.cell.2019.01.043
6. Pappalardo XG, Barra V (2021) Losing DNA methylation at repetitive elements and breaking bad. Epigenetics Chromatin 14:25. https://doi.org/10.1186/s13072-021-00400-z
7. Carollo PS, Barra V (2023) Chromatin epigenetics and nuclear lamina keep the nucleus in shape: examples from natural and accelerated aging. Biol Cell 115:e2200023. https://doi.org/10.1111/boc.202200023
8. Martino S, Carollo PS, Barra V (2023) A glimpse into chromatin organization and nuclear lamina contribution in neuronal differentiation. Genes (Basel) 14:1046. https://doi.org/10.3390/genes14051046
9. Jackson-Grusby L, Laird PW, Magge SN et al (1997) Mutagenicity of 5-aza-2'-deoxycytidine is mediated by the mammalian DNA methyltransferase. Proc Natl Acad Sci U S A 94:4681–4685. https://doi.org/10.1073/pnas.94.9.4681
10. Unterberger A, Andrews SD, Weaver ICG, Szyf M (2006) DNA methyltransferase 1 knockdown activates a replication stress checkpoint. Mol Cell Biol 26:7575–7586. https://doi.org/10.1128/MCB.01887-05
11. Hollenbach PW, Nguyen AN, Brady H et al (2010) A comparison of azacitidine and decitabine activities in acute myeloid leukemia cell lines. PLoS ONE 5:e9001. https://doi.org/10.1371/journal.pone.0009001
12. Barra V, Schillaci T, Lentini L et al (2012) Bypass of cell cycle arrest induced by transient DNMT1 post-transcriptional silencing triggers aneuploidy in human cells. Cell Div 7:2. https://doi.org/10.1186/1747-1028-7-2
13. Costa G, Barra V, Lentini L et al (2016) DNA demethylation caused by 5-Aza-2'-deoxycytidine induces mitotic alterations and aneuploidy. Oncotarget 7(3):726–3739. https://doi.org/10.18632/oncotarget.6897
14. Kaji K, Factor VM, Andersen JB et al (2016) DNMT1 is a required genomic regulator for murine liver histogenesis and regeneration. Hepatology 64:582–598. https://doi.org/10.1002/hep.28563
15. Tang D, Zheng S, Zheng Z et al (2022) Dnmt1 is required for the development of auditory organs via cell cycle arrest and Fgf signalling. Cell Prolif 55:e13225. https://doi.org/10.1111/cpr.13225
16. Laranjeira ABA, Hollingshead MG, Nguyen D et al (2023) DNA damage, demethylation and anticancer activity of DNA methyltransferase (DNMT) inhibitors. Sci Rep 13:5964. https://doi.org/10.1038/s41598-023-32509-4
17. Li E, Bestor TH, Jaenisch R (1992) Targeted mutation of the DNA methyltransferase gene results in embryonic lethality. Cell 69:915–926. https://doi.org/10.1016/0092-8674(92)90611-f
18. Liao J, Karnik R, Gu H et al (2015) Targeted disruption of DNMT1, DNMT3A and DNMT3B in human embryonic stem cells. Nat Genet 47:469–478. https://doi.org/10.1038/ng.3258
19. DNMT1 DepMap Gene Summary. https://depmap.org/portal/gene/DNMT1?tab=overview. Accessed 25 Feb 2024
20. Zhang Z, Wang G, Li Y et al (2022) Recent progress in DNA methyltransferase inhibitors as anticancer agents. Front Pharmacol. https://doi.org/10.3389/fphar.2022.1072651
21. Palii SS, Van Emburgh BO, Sankpal UT et al (2008) DNA methylation inhibitor 5-Aza-2′-deoxycytidine induces reversible genome-wide DNA damage that is distinctly influenced by DNA methyltransferases 1 and 3B. Mol Cell Biol 28:752–771. https://doi.org/10.1128/MCB.01799-07
22. Qi D, Li J, Que B et al (2016) Long non-coding RNA DBCCR1-003 regulate the expression of DBCCR1 via DNMT1 in bladder cancer. Cancer Cell Int 16:81. https://doi.org/10.1186/s12935-016-0356-8
23. Wang X-Z, Cheng Y, Wang K-L et al (2016) Peperomin E reactivates silenced tumor suppressor genes in lung cancer cells by inhibition of DNA methyltransferase. Cancer Sci 107:1506–1519. https://doi.org/10.1111/cas.13029
24. Amatori S, Papalini F, Lazzarini R et al (2009) Decitabine, differently from DNMT1 silencing, exerts its antiproliferative activity through p21 upregulation in malignant pleural mesothelioma (MPM) cells. Lung Cancer 66:184–190. https://doi.org/10.1016/j.lungcan.2009.01.015
25. Tsujioka T, Yokoi A, Uesugi M et al (2013) Effects of DNA methyltransferase inhibitors (DNMTIs) on MDS-derived cell lines. Exp Hematol 41:189–197. https://doi.org/10.1016/j.exphem.2012.10.006
26. Chen T, Hevi S, Gay F et al (2007) Complete inactivation of DNMT1 leads to mitotic catastrophe in human cancer cells. Nat Genet 39:391–396. https://doi.org/10.1038/ng1982
27. Rhee I, Jair K-W, Yen R-WC et al (2000) CpG methylation is maintained in human cancer cells lacking DNMT1. Nature 404:1003–1007. https://doi.org/10.1038/35010000
28. Jiang C, Gong F (2016) DNA methyltransferase 1: a potential gene therapy target for hepatocellular carcinoma? Oncol Res Treat 39:448–452. https://doi.org/10.1159/000447414

29. Milutinovic S, Zhuang Q, Niveleau A, Szyf M (2003) Epigenomic stress response. Knockdown of DNA methyltransferase 1 triggers an intra-S-phase arrest of DNA replication and induction of stress response genes. J Biol Chem 278:14985–14995. https://doi.org/10.1074/jbc.M213219200
30. Wang H, Wu J, Meng X et al (2011) MicroRNA-342 inhibits colorectal cancer cell proliferation and invasion by directly targeting DNA methyltransferase 1. Carcinogenesis 32:1033–1042. https://doi.org/10.1093/carcin/bgr081
31. Snyder RD, Lachmann PJ (1989) Differential effects of 5-azacytidine and 5-azadeoxycytidine on cytotoxicity, DNA-strand breaking and repair of X-ray-induced DNA damage in HeLa cells. Mutat Res 226:185–190. https://doi.org/10.1016/0165-7992(89)90018-3
32. Scelfo A, Barra V, Abdennur N et al (2024) Tunable DNMT1 degradation reveals DNMT1/DNMT3B synergy in DNA methylation and genome organization. J Cell Biol 223:e202307026. https://doi.org/10.1083/jcb.202307026
33. Nishimura K, Yamada R, Hagihara S et al (2020) A super-sensitive auxin-inducible degron system with an engineered auxin-TIR1 pair. Nucleic Acids Res 48:e108. https://doi.org/10.1093/nar/gkaa748
34. Holland AJ, Fachinetti D, Han JS, Cleveland DW (2012) Inducible, reversible system for the rapid and complete degradation of proteins in mammalian cells. Proc Natl Acad Sci U S A 109:E3350-3357. https://doi.org/10.1073/pnas.1216880109
35. Carollo PS, Tutone M, Culletta G et al (2023) Investigating the inhibition of FTSJ1, a tryptophan tRNA-specific 2′-O-methyltransferase by NV TRIDs, as a mechanism of readthrough in nonsense mutated CFTR. Int J Mol Sci 24:9609. https://doi.org/10.3390/ijms24119609
36. Giacomini G, Piquet S, Chevallier O et al (2024) Aberrant DNA repair reveals a vulnerability in histone H3.3-mutant brain tumors. Nucleic Acids Res 52:2372–2388. https://doi.org/10.1093/nar/gkad1257
37. Said M, Barra V, Balzano E et al (2022) FANCD2 promotes mitotic rescue from transcription-mediated replication stress in SETX-deficient cancer cells. Commun Biol 5:1395. https://doi.org/10.1038/s42003-022-04360-2
38. Perriera R, Vitale E, Pibiri I et al (2023) Readthrough approach using NV translational readthrough-inducing drugs (TRIDs): A Study of the Possible Off-Target Effects on Natural Termination Codons (NTCs) on TP53 and Housekeeping Gene Expression. Int J Mol Sci 24:15084. https://doi.org/10.3390/ijms242015084
39. Veneziano L, Barra V, Lentini L et al (2016) p14(ARF) prevents proliferation of aneuploid cells by inducing p53-dependent apoptosis. J Cell Physiol 231:336–344. https://doi.org/10.1002/jcp.24976
40. Veneziano L, Barra V, Cilluffo D, Di Leonardo A (2019) Proliferation of aneuploid cells induced by CENP-E depletion is counteracted by the p14ARF tumor suppressor. Mol Genet Genomics 294:149–158. https://doi.org/10.1007/s00438-018-1495-5
41. Barra V, Chiavetta RF, Titoli S et al (2022) Specific irreversible cell-cycle arrest and depletion of cancer cells obtained by combining curcumin and the flavonoids quercetin and fisetin. Genes 13:1125. https://doi.org/10.3390/genes13071125
42. Aparicio T, Megías D, Méndez J (2012) Visualization of the MCM DNA helicase at replication factories before the onset of DNA synthesis. Chromosoma 121:499–507. https://doi.org/10.1007/s00412-012-0381-x
43. Shin H, Leung A, Costello KR et al (2023) Inhibition of DNMT1 methyltransferase activity via glucose-regulated O-GlcNAcylation alters the epigenome. Elife 12:e85595. https://doi.org/10.7554/eLife.85595
44. Young JI, Smith JR (2001) DNA methyltransferase I (DNMT1) inhibition induces a p21 dependent cell cycle arrest. ScientificWorldJournal 1:131. https://doi.org/10.1100/tsw.2001.232
45. Milutinovic S, Brown SE, Zhuang Q, Szyf M (2004) DNA methyltransferase 1 knock down induces gene expression by a mechanism independent of DNA methylation and histone deacetylation. J Biol Chem 279:27915–27927. https://doi.org/10.1074/jbc.M312823200
46. Shieh S-Y, Ikeda M, Taya Y, Prives C (1997) DNA damage-induced phosphorylation of p53 alleviates inhibition by MDM2. Cell 91:325–334. https://doi.org/10.1016/S0092-8674(00)80416-X